

# FOSSIL RADIO PLASMA IN CLUSTER MERGER SHOCK WAVES

T.A. ENSSLIN<sup>1</sup>, M. BRÜGGEN<sup>1,2</sup>

<sup>1</sup> *Max-Planck-Institut für Astrophysik, Garching D-85741, Germany*

<sup>2</sup> *Institute of Astronomy, Madingley Road, Cambridge CB3 0HA, United Kingdom*

In several merging clusters of galaxies so-called *cluster radio relics* have been observed. These are extended radio sources which do not seem to be associated with any radio galaxy. Two competing physical mechanisms to accelerate the radio emitting electrons have been proposed: (i) diffusive shock acceleration and (ii) adiabatic compression of fossil radio plasma by merger shock waves. Here the second scenario is investigated. We present detailed 3-dimensional magneto-hydrodynamical simulations of the passage of a radio plasma cocoon through a shock wave. Taking into account synchrotron, inverse Compton and adiabatic energy losses and gains we evolved the relativistic electron population to produce synthetic radio maps in Stokes I-, Q-, and U-polarisation. In the synthetic radio maps the electric polarisation vectors are mostly perpendicular to the filamentary radio structures.

## 1 Introduction

In the current picture of hierarchical structure formation clusters of galaxies grow mainly by the merging of smaller and moderately sized sub-clusters. During such merger events a significant fraction of the kinetic energy of the intergalactic medium (IGM) is dissipated in Mpc-sized shock waves. The shock waves are responsible for heating the IGM to temperatures of several keV. Moreover, they are likely to inject and accelerate relativistic particle populations on cluster scales.

Cluster-wide relativistic electron populations are indeed observed in several merging or post-merging clusters. The so-called *cluster radio relics* are believed to be directly related to cluster mergers (Enßlin et al. 1998, Roettiger et al. 1999, Venturi et al. 1999, Enßlin & Gopal-Krishna 2001). Like the radio halos they are extended radio sources with a steep spectrum. In the literature radio relics are often confused with radio halos even though several distinctive properties exist. Cluster radio relics are typically located near the periphery of the cluster; they often exhibit sharp emission edges and many of them show strong radio polarisation.

In several cases it could be shown that shock waves are present at the locations of the relics. Moreover, the cluster radio relic 1253+275 in the Coma cluster shows a morphological connection to the nearby radio galaxy NGC 4789 (Giovannini, Feretti & Stanghellini 1991). This suggests that radio relics may be fossil radio plasma that has been revived by a shock. Fossil radio plasma is the former outflow of a radio galaxy in which the high-energy radio emitting electrons have lost their energy. Due to their invisibility in the radio these cocoons are also called *radio ghosts* (Enßlin 1999).

The first relic formation models considered diffusive shock acceleration (Fermi I) as the process producing the radio emitting electrons (Enßlin et al. 1998, Roettiger et al. 1999, Venturi et al. 1999). However, when a fossil radio cocoon is passed by a cluster merger shock

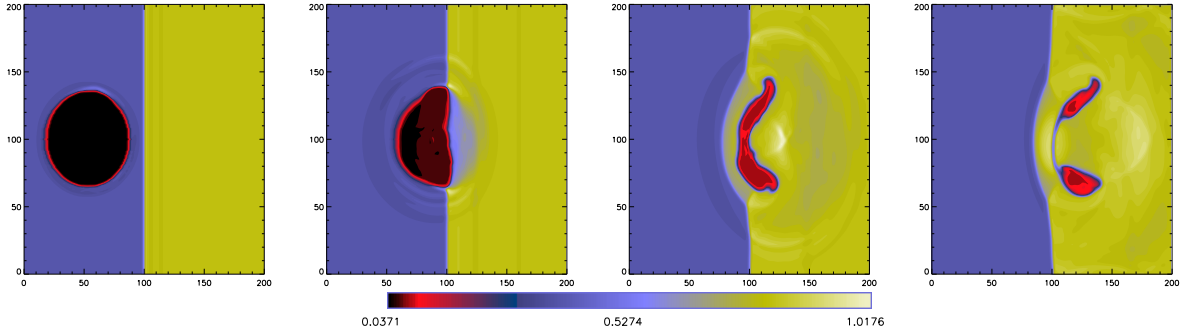


Figure 1: Evolution of the gas density in a central slice through the simulation volume. The formation of a torus is visible.

wave, with a typical velocity of a few 1000 km/s, the cocoon is compressed adiabatically and not shocked, owing to the much higher sound speed within it. Therefore, shock acceleration cannot be the mechanism that re-energises the relativistic electron population in the cocoon. But the energy gained during the adiabatic compression combined with the increase in the magnetic fields strength can make a fossil radio cocoon emit radio waves again. One prerequisite for this is that the electron population is not older than 0.2 - 2 Gyr (Enßlin & Gopal-Krishna 2001).

Enßlin & Gopal-Krishna (2001) showed that the spectral properties of cluster radio relics are well reproduced by this scenario. Here and in Enßlin & Brüggén (2001), we demonstrate that the observed morphologies and polarisation patterns are reproduced by this model as well. This is done with the help of the first 3-dimensional magneto-hydrodynamical (MHD) simulations of a fossil radio cocoon that is passed by a shock wave. We produce artificial radio maps that can be compared directly to new high-resolution radio maps of cluster radio relics.

## 2 Method

### 2.1 3D MHD Simulation

The magneto-hydrodynamical simulations were obtained using the ZEUS-3D code which was developed especially for problems in astrophysical hydrodynamics (Stone & Norman 1992a, b).

The simulations were computed on a Cartesian grid with  $100^3$  and  $200^3$  equally spaced zones. In the units of the simulation the computational domain ranged from 0 to 10 in each coordinate. The simulation was set up such that a stationary shock formed at  $x = 5$  that is perpendicular to the direction of the flow.

In the pre-shock region a spherical bubble was set up, in which the density was lowered by a factor of 10 with respect to the environment. In turn, the temperature in the bubble was raised such that the bubble remained in pressure equilibrium with its surroundings. Inside the bubble a magnetic field was set up which was computed from a random field that consisted of several hundred Fourier modes. Finally, the bubble was filled with around  $10^4$  uniformly distributed tracer particles that are advected with the flow.

### 2.2 Radio Maps

The radio maps are constructed using the tracer particles. Initially, each tracer particle is located inside the radio plasma cocoon and is associated with the same initial relativistic electron population. Then the electron spectrum for each tracer particle is evolved in time taking into account synchrotron, inverse Compton, and adiabatic energy losses and gains (see Enßlin & Gopal-Krishna 2001).

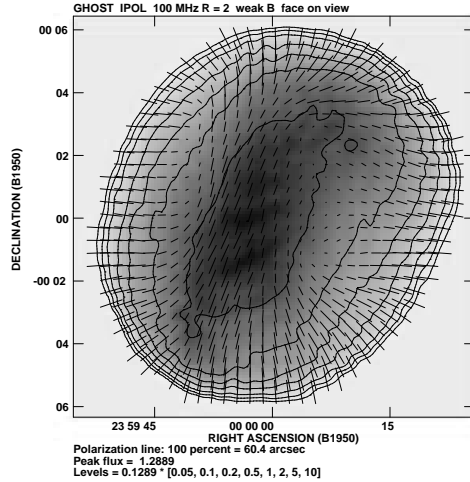


Figure 2: Radio emission of the radio bubble before shock passage. The shock has a compression factor of  $C = 2$ . The polarisation E-vectors are displayed by dashes with the length proportional to the relative polarisation. Here and in the following radio maps the flux is given in Jansky per simulation pixel (with linear size of 20.6 arcsec)

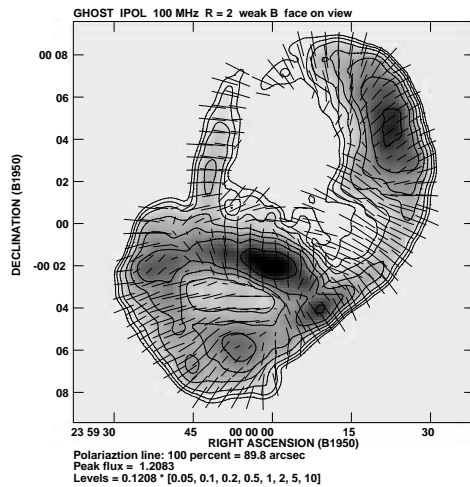


Figure 3: Same as Fig. 2. Late stage of the shock passage in the same model.

The pre-shock external gas density is set to about  $5 \cdot 10^{-4}$  electrons/cm<sup>3</sup> and the temperature to 1-2 keV. The simulation box is assumed to have a size of 1 Mpc<sup>3</sup> and to be located at a distance of 100 Mpc from the observer.

An increase in the radio luminosity during the compression can be seen in the simulation. However, the strong increase expected from the analytical model of Enßlin & Gopal-Krishna (2001) could not be reproduced here. This is a result of the decaying magnetic fields due to numerical resistivity, and not a failure of the model. In order not to be too much affected by the rapidly evolving spectral cutoff we restrict our analysis in the following to a low radio frequency, namely 100 MHz.

### 2.3 Radio Morphology

As the shock wave passes the initially spherical radio cocoon (Fig. 2), the cocoon is torn into a filamentary structure (Fig. 3). In the simulations with weak magnetic fields the final morphology

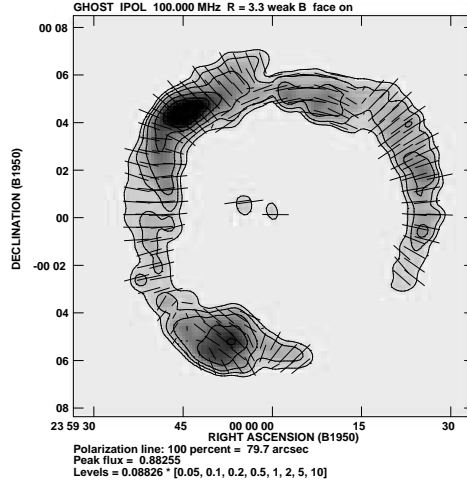


Figure 4: Edge-on view of the late stage of the shock passage in a model, where the shock has a compression factor of  $C = 3.3$ . Note the reversal of the polarization vector orientation. For details see Fig. 2.

is toroidal for a strong shock, Fig. 4, and shows two tori in the case of a weak shock wave, Fig. 3). Such a double torus seems to be observed in the relic in Abell 85 (Slee et al. 2001). The degree of polarisation is relatively high everywhere. The electric polarisation vectors tend to be perpendicular to the radio filaments indicating aligned magnetic field structures within them. At some few spots the polarisation E-vectors are aligned with the radio filaments (see Fig. 4).

#### 2.4 Radio Polarisation

The total integrated polarisation flux of a radio relic observed face-on can be expected to be small. In the case of a toroidal relic all polarisation orientations are roughly equally present and therefore cancel each other out in the surface integration. But even in a more complex relic the polarisation cancels out in the face-on view.

In the edge-on view this is different. Now a preferential direction exists: E-vectors tend to be aligned with the projected shock normal. Whenever the imprinted polarisation dominates over the initial intrinsic one, the direction of the E-vector can be used relatively reliably to infer the shock normal projected onto the plane of the sky. The angle with respect to this plane can be estimated roughly from the total polarisation.

Thus, in principle, the 3-dimensional orientation (modulo a mirror ambiguity) can be derived from the polarisation data only. However, these points will need additional investigations before it is applicable to real data.

#### 2.5 Shock Properties

The observed dimensions of a cluster radio relic with a toroidal shape can be used to get a rough estimate of the shock strength. This is based on the observation that in the numerical simulations the diameter  $D$  of the spherical cocoon and the major radius of the torus after the passage of the shock are approximately equal. Since the major and minor radii of the torus can be read off approximately from a sensitive high-resolution radio map, the compression of the radio plasma by the shock can be estimated. In the idealised case of an initially spherical and finally toroidal radio cocoon, the compression factor is given by

$$C = \frac{V_{\text{sphere}}}{V_{\text{torus}}} = \frac{2D^2}{3\pi d^2}. \quad (1)$$

Using Eq. (12), the shock strength can be estimated. Assuming the radio cocoon to be in pressure equilibrium with its environment before and after the shock passage, the pressure jump in the shock is given by  $P_2/P_1 = C^{\gamma_{\text{rp}}}$ . If the adiabatic index of the radio plasma  $\gamma_{\text{rp}}$  is assumed to be known, e.g.  $\gamma_{\text{rp}} = 4/3$  for an ultra-relativistic equation of state, the shock strength can be estimated. But even if this assumption is not justified and the geometry deviates from the idealised geometries assumed here, the strength of the shock wave should be correlated to the ratio of the global diameter of a toroidal relic and the thickness of its filaments. Unfortunately, the quality of the best current radio maps of relics do not yet allow a qualitative comparison of the shock strength by comparing the  $D/d$  ratios of toroidal relics. But these maps demonstrate that the necessary sensitivity and resolution might be reached soon.

If, furthermore, the strength of the shock wave of well resolved cluster radio relics can be estimated independently from X-ray maps of the IGM, it would be possible to directly measure the adiabatic index of radio plasma. Even though the present radio and X-ray data do not have the required accuracy yet, this method will enable us to measure the unknown equation of state of radio plasma in the future.

In our simulations the adiabatic index of the radio plasma ( $\gamma_{\text{rp}} = \gamma_{\text{gas}} = 5/3$ ) and the shock strength are known ( $P_2/P_1 = 3.5$  and  $P_2/P_1 = 17.4$  for the shock compression factor  $C_{\text{shock}} = 2$  and  $C_{\text{shock}} = 3.3$  respectively). Thus we find that the ratio of the length scales  $D/d \approx 3$  for  $C_{\text{shock}} = 2$  and  $D/d \approx 5$  for  $C_{\text{shock}} = 3.3$ . This is roughly consistent with our synthetic radio maps. At least the qualitative correlation of shock strength and diameter ratio is clearly observed, as can be seen in Figs. 3 and 4.

### 3 Conclusion

We have presented 3-D MHD simulations of a hot, magnetised bubble that traverses a shock wave in a much colder and denser environment. This is assumed to be a fair model for a blob of radio plasma in the IGM which is passed by a cluster merger shock wave. We have calculated radio polarisation maps for the relativistic electron population and computed the spectrum subject to synchrotron-, inverse Compton- and adiabatic energy losses and gains. These maps show that the shock wave produces filamentary radio emitting structures and, in many cases, toroidal structures. Such filaments and tori are indeed observed by very recent high-resolution radio maps of cluster radio relics (Slee et al. 2001). Our simulations find polarisation patterns which indicate that the magnetic fields are mostly aligned with the direction of the filaments. This also seems to be the case for the observed cluster radio relics.

Therefore, we conclude that we have found strong evidence that cluster radio relics indeed consist of fossil radio plasma that has been compressed adiabatically by a shock wave, as proposed by Enßlin & Gopal-Krishna (2001).

The formation of the tori and filaments is not instantaneous. First, the simulations show a phase in which the radio plasma is strongly compressed into a flat shape. During this phase a sheet-like radio relic with a flat spectrum would be observed. Later, the radio plasma moves towards the edges of this sheet and finally becomes a torus (or a more complicated, filamentary structure). Since spectral ageing is likely to have affected these later stages, we expect that on average the filamentary relics have a steeper, more bent radio spectrum than the sheet-like ones.

Our simulations indicate that the diameter  $D$  of the bubble of radio plasma remains approximately constant during the passage of the shock. It was also found that the final structure consists of radio filaments of small diameter  $d$  that are distributed (often in form of a torus) in a region of size  $D$ . The compression factor of the radio plasma is proportional to  $(D/d)^2$ , and this ratio is a measure of the shock strength. Thus, the approximate compression factor of the radio plasma can be read off the radio map. The local radio polarisation strongly reflects the complicated magnetic field structures while the total integrated polarisation of a relic re-

veals the 3-dimensional orientation of the shock wave. Since the compression aligns the fields with the shock plane, the sky-projected field distribution is aligned with the intersection of the shock plane and the sky plane. Thus, the direction of the total E-polarisation vector yields the sky-projected normal of the shock wave. The angle between the normal of the shock and the plane of the sky can in principle be estimated from the fractional polarisation of the integrated flux. We conclude that this work provides strong evidence that cluster radio relics are revived bubbles of fossil radio plasma, the so-called *radio ghosts*. Spectral aging arguments (Enßlin & Gopal-Krishna 2001) predict the existence of a sizable population of yet undetected cluster radio relics which are only observable with sensitive low frequency radio telescopes. More details of the simulations can be found in Enßlin & Brüggen (2001).

## Acknowledgments

We thank O.B. Slee, A.L. Roy, M. Murgia, H. Andernach, M. Ehle for providing us with their observational data prior to publication, and allowing us to display their 1.4 GHz map of the relic in Abell 85. We also thank G. Giovannini and L. Feretti for access to their 330 MHz data of the same relic. We acknowledge A. Kercek's contributions to a very early stage of this simulation project. Some of the computations reported here were performed using the UK Astrophysical Fluids Facility (UKAFF). This work was supported by the European Community Research and Training Network 'The Physics of the Intergalactic Medium'. TAE and MB acknowledge the award of a European grant to attend this excellent conference.

## References

1. T.A. Enßlin, M. Brüggen, MNRAS, submitted, 2001.
2. T.A. Enßlin in *Diffuse Thermal and Relativistic Plasma in Galaxy Clusters*, eds. H. Böhringer, L. Feretti, P. Schücker, 275, astro-ph/9906212. (1999)
3. T.A. Enßlin, Gopal-Krishna, A&A **366**, 26 (2001).
4. T.A. Enßlin, P.L.Biermann, U. Klein, S. Kohle, A&A **332**, 395 (1998).
5. L. Feretti, In IAU Symp. 199, 'The Universe at Low Radio Frequencies'. astro-ph/0006379 (1999).
6. G. Giovannini, L. Feretti, C. Stanghellini, A&A **252**, 528 (1991).
7. K. Roettiger, J.O. Burns, J.M. Stone, ApJ **518**, 603 (1999).
8. O.B. Slee, A.L. Roy, M. Murgia, H. Andernach, M. Ehle, AJ , submitted (2001)
9. J.M. Stone, M.L. Norman, APJS **80**, 753 (1992a).
10. J.M. Stone, M.L. Norman, 1992b, APJS **80**, 791 (1992b).
11. T. Venturi, S. Bardelli, G. Zambelli, R. Morganti, R.W. Hunstead, in *Diffuse Thermal and Relativistic Plasma in Galaxy Clusters*, eds. H. Böhringer, L. Feretti, P. Schücker, 27 (1999)